ISBN: 978-3-95450-233-2 ISSN: 2673-5504 doi:10.18429/JACoW-SRF2021-SUPCAV002

EX-SITU INVESTIGATION OF THE EFFECTS OF HEATING RATE ON THE RECRYSTALLIZATION IN ROLLED POLYCRYSTALS OF HIGH-PURITY NIOBIUM*

Z.L. Thune†,T.R. Bieler, N. Fleming, C. McKinney, E.M. Nicometo
Michigan State University, East Lansing, MI, USA
S. Balachandran
Applied Superconductivity Center, Florida State University, Tallahassee, FL, USA

Abstract

The consistent production of high-purity niobium cavities for superconducting radio frequency (SRF) applications is crucial for enabling improvements in accelerator performance. Recent work has shown that dislocations and grain boundaries trap magnetic flux which dissipates energy and degrades cavity performance. We hypothesize that the current heating rate used in production is too slow and therefore facilitates recovery rather than recrystallization. Recovery, unlike recrystallization, does not reduce the number of geometrically necessary dislocations (GNDs) that are strongly correlated to trapped magnetic flux. Using excess high-purity niobium saved from the production of a cavity, the material was divided into two groups and rolled to ~30% reduction with half rolled parallel to the original rolling direction, and the other half rolled perpendicular. To examine the effect of heating rate, samples were encapsulated in quartz tubes and placed into either a preheated furnace or a cold furnace to allow for heat treatments at different rates. Then using ex-situ electron backscatter diffraction (EBSD) mapping, the extent of recrystallization was determined.

INTRODUCTION

Ensuring that the SRF cavities produced from high-purity niobium have a high Q value is of great importance in the production of the cavities. Degradation in the Q value is associated with a number of factors: such as the introduction of new dislocation substructures due to the deformation required to form the cavities; the possibility of introducing impurities (specifically hydrogen and the resulting niobium hydrides) through the necessary cryo-temperature cooling of the cavities; as well as recovery, recrystallization, and grain growth due to the heat treatments imposed on the cavity post production. There is significant current interest in the impact of trapped flux which is associated with defects in the metal such as dislocations [1–4]. With current heat treatment schedules, dislocation recovery (reduction in dislocation density with formation of low energy low angle grain boundaries within in the deformed grains) may occur as much as recrystallization (motion of high angle grain boundaries that result in a nearly perfect crystal structure behind them) [5]. As low angle boundaries have been shown to trap flux as effectively as high angle grain boundaries when they are parallel to the magnetic field, it is reasonable to expect that the probability of a boundary being parallel to a magnetic field will be much greater if grains have a network of low angle boundaries within them. Consequently, recrystallization is highly desirable. Recent work has shown that higher temperature heat treatments reduce flux pinning losses in cavities, and as this higher temperature favors more grain growth, fewer low angle boundaries are present. On the other hand, the cavities require sufficient strength as a pressure vessel [6], so the grain size should not become too large. Therefore, a more complete understanding of recrystallization in deformed high-purity niobium and its ties to the dislocation substructure resulting from forming, specifically the geometrically necessary dislocations (GNDs) that become low angle boundaries, it will be possible to identify production specifications for both cost-effective and high Q niobium SRF cavities [7].

Furthermore, the variability of rolled niobium sheet metal is know to be large, as microstructures and local texture gradients are highly variable from one batch of material to the next even for the same product from the same supplier. Thus, the current acceptance criteria based upon grain size and yield strength may not be sufficient to ensure that recrystallization occurs in formed cavities in a predictable way. Therefore, it would be valuable to determine if a small sample of a batch of material will meet a minimum recrystallization threshold. One of the simplest ways to do this is with small samples that are deformed in a easily reproducible way, to determine the fraction recrystallized in a reproducible and robust manner. To this end, this paper examines a particular deformation history of sheet using a ~30% reduction, and different heat treatment strategies are compared. An operating hypothesis examined in this paper is that a slow heating rate facilitates recovery that removes excess dislocations by the time that the heat treatment temperature is reached. Therefore, if the material is heated faster, there may be more dislocations still present by the time the heat treatment temperature is reached, such that the driving force for recrystallization may be increased, and hence the fraction recrystallized is increased. A critical enabling metric to assess this hypothesis is the measurement of the fraction recrystallized, and this paper compares several thresholds and methods to make this assessment.

* This work is supported by US Dept. of Energy award DE-SC0009960
† thunezac@msu.edu

ISBN: 978-3-95450-233-2 ISSN: 2673-5504 doi:10.18429/JACoW-SRF2021-SUPCAV002

SAMPLE PREPARATION AND EXPERIMENTAL PROCEDURE

The source material used in this study was selected from the excess of a high purity niobium sheet produced by Tokyo Denkai, which was used in the fabrication of end-caps for low beta cavities at the Facility for Rare Isotope Beams (FRIB) at Michigan State University. The creation of coupon samples illustrated in Fig. 1, began with removing the narrow parts of the piece and then cold-rolling the nearly square sample in the same direction as the initial rolling direction of the sheet to ~30% reduction in 3 passes using a laboratory rolling mill with 100 mm rolls. Once the rolling was completed, electrical discharge machining (EDM) was used to cut 10 samples from the rolled piece and one sample from the as-received piece adjacent to the rolled material to provide an undeformed sample to provided a basis for comparison. The rolled samples have the approximate dimensions of 2.5mm x 14mm x 10mm. All of the samples were then chemically polished using a buffered chemical polishing (BCP) solution to remove 10-15μm of material, to ensure removal of the EDM recast surface. Further mechanical polishing was necessary to obtain suitable electron backscattered diffraction (EBSD) patterns. Then a cross-sectional face parallel with the rolling direction of the sample was mechanically polished with a vibratory polishing machine with 0.05μm colloidal silica suspension for ~24hours until a mirror finish had been achieved which allowed for EBSD data to be obtained using a TESCAN Mira SEM with a TSL OIM system (Malwah NJ). To facilitate this polishing process, mounts were fabricated using a polymer 3-D printing process so that four samples could be easily inserted and removed from the clamp shown in Fig. 2.

Four of the samples from the same column were used for this study. After initial EBSD scans were taken across the full width of the cross-sectional face, the samples were encapsulated in evacuated quartz tubes and heat treated under different conditions; two samples were heat treated at 1000°C for 3 hours and the other two were heat treated at 900°C for 3 hours. From each pair, 1 was heated with a standard 3 hour heating ramp from room temperature (~25°C)

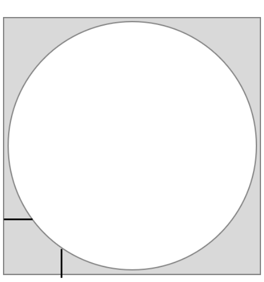

(a) Initial excess material and representative corner cut into 3 pieces.

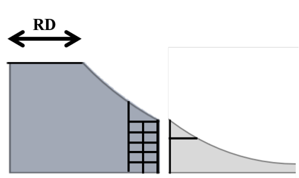

(b) Corner piece (darker grey) rolled to ~30% reduction (in the direction noted above) and all of the samples cut from the edge of rolled piece as well as the neighboring as-received piece.

Figure 1: Images representing the creation of coupon samples used in this study.

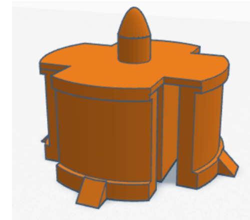

Figure 2: The 3D printed mount used to hold 4 samples at a time for polishing. Once the samples are placed into the mount, a hose clamp is used to secure them.

prior to the 3 hour hold at temperature, and the other was inserted into the furnace during the 3 hour heating ramp at ~90% of the hold temperature to ensure a faster heating rate. After the heat treatments were completed, EBSD scans were obtained from approximately the same locations on each sample to provide an accurate comparison data set such that the regions scanned on two adjacent samples were within a few mm of each other.

RESULTS AND DISCUSSION

The effect of the rolling and subsequent heat treatments has a significant effect on the microstructure of the material, as illustrated in the inverse pole figure (IPF) maps in Fig. 3. The initial material has fine grains which are each fairly uniform in size and evenly distributed among their preferred orientations. Cold rolling the material stretches them in the rolling direction as well as introduces a significant amount of orientation spread within the individual grains. With the 900°C and 1000°C heat treatments the microstructure underwent some level of recrystallization and grain growth; however the grain shape is more uniform and larger in the 1000°C heat treatment, in agreement with recent work stating that the higher temperature heat treatments can lead to a more desirable microstructure for SRF applications.

GND Density and Recrystallization

For this study, a critical points is to understand how heat treatment affects the GND density in the material and to investigate the heating rate and temperature in relation to recrystallization. GND density plots are available in the OIM Analysis software. The software calculates this based on a set of applicable slip systems and then calculates the values based on grain orientation and overall distortion of the EBSD patterns. While this can be a usefull metric, a number of factors associated with the imaging process can influence the final outcome. With this in mind, the default settings were used for GND density calculations and the resulting plot(s) are in Fig. 4.

While it is evident from Fig. 4 that the as-recieved GND density was generally in the range of 1-10$*10^{12}$/m^2, the rolled state pushed the GND densities up to the 10-100$*10^{12}$/m^2. This was expected with the introduction of dislocations due to the deformation of material. Once theses two states were measured it provided a basis for comparing

ISBN: 978-3-95450-233-2 ISSN: 2673-5504 doi:10.18429/JACoW-SRF2021-SUPCAV002

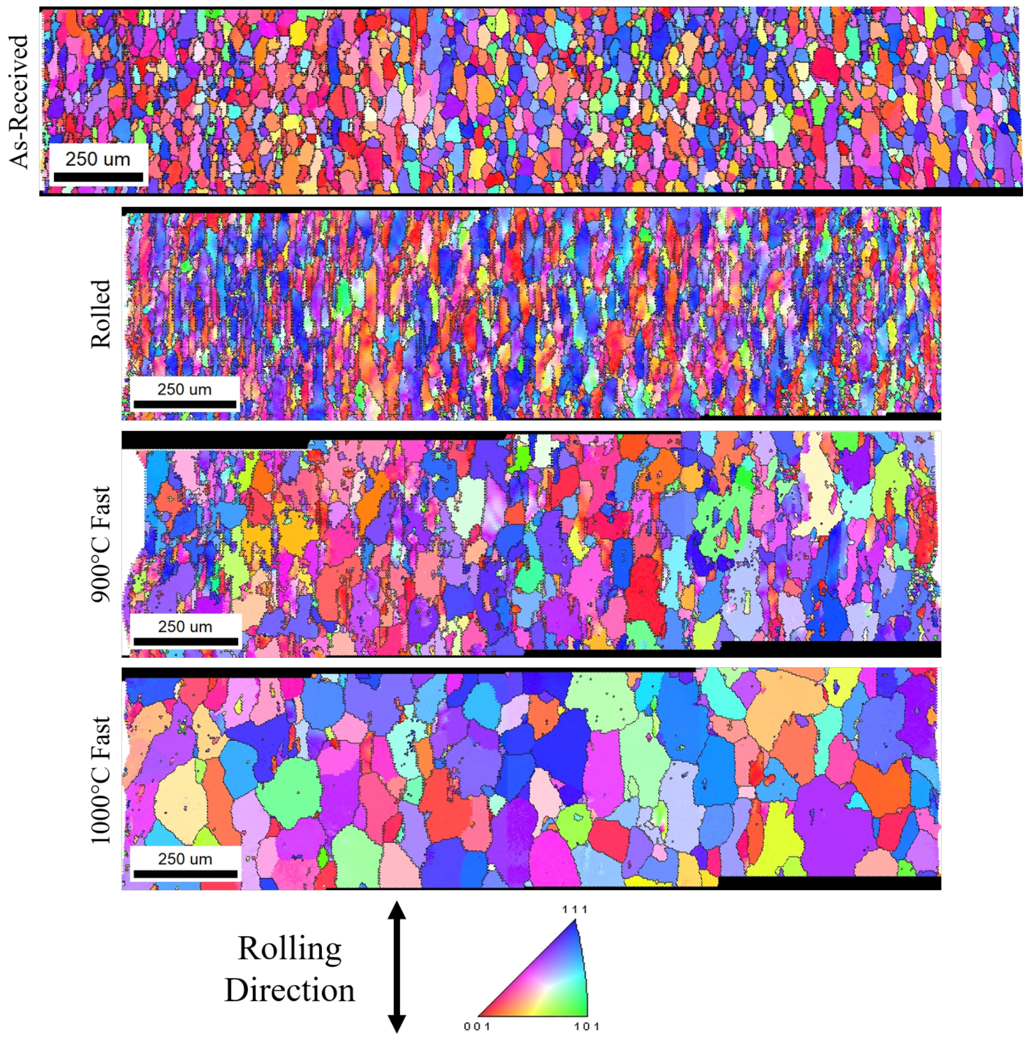

Figure 3: IPF maps (and legend) of the niobium microstructure(s) investigated in relation to the heat treatment imposed. The rolling direction is vertical, and the width is the full thickness of the sheet.

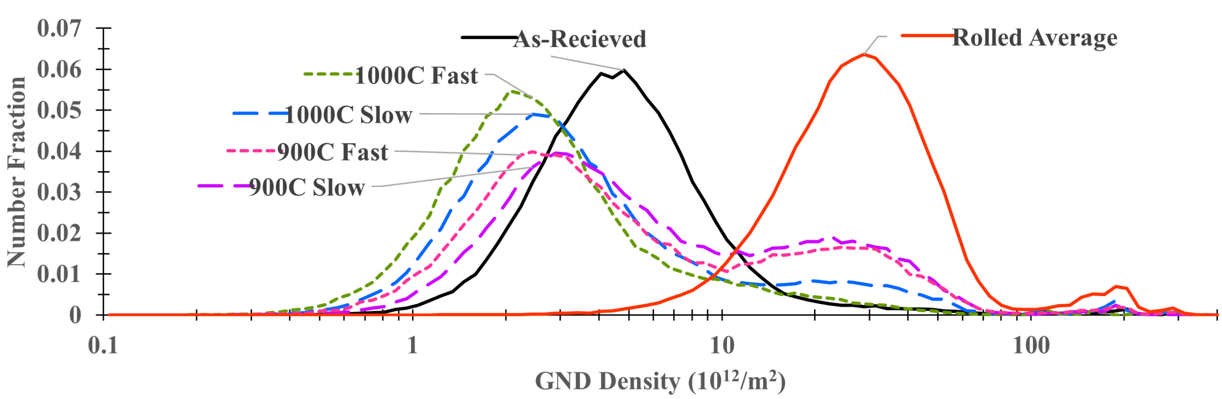

Figure 4: The GND density of each of the heat treated samples as well as the As-Received and an average of all of the as-rolled sample measurements.

ISBN: 978-3-95450-233-2 ISSN: 2673-5504 doi:10.18429/JACoW-SRF2021-SUPCAV002

Table 1: GND Density Below the Annealed State Cutoff Density: $10 * 10^{12}/m^2$

Sample	Percent of GND Density
As-Received	89
Rolled	5
1000C Slow	84
1000C Fast	91
900C Slow	68
900C Fast	71

the changes caused by the different heat treatments. While the largest peak for each sample is in a similar range to the as-recieved condition, showing a significant reduction in the GND density there are clear differences among the heat treatments. In both the 900°C and the 1000°C fast heat treatments the peak in the lower GND density range was shifted to the left (lower density) of its slow (standard) heat treatment counterpart. This shows that regardless of the recrystallization in the system the average GND density of the fast heating rate decreases the GND density more effectively than the slow heating rate. It is also evident in the 1000°C heat treatments that the fast heating rate reduces the GND density more in the higher density range associated with the rolled condition, leading to what appears to be a more uniform reduction in the overall GND density. This is not the case with the 900°C heat treatments though as hige density peaks from the two heating rates are nearly identical in shape, the only noticeable difference is the leftward shift in the fast heating rate in the low dislocation density range that mirrors the 1000°C fast heating rate.

While the peaks seem to confirm a piece of our working hypothesis, it is necessary to evaluate the level of recrystallization in the system as well. However, based on the significant correlation of peaks between the as-received or rolled states and the resulting annealed material(s) a GND fraction was calculated based on the GND density above and below $10*10^{12}/m^2$ to allow for comparison to the recrystallization fractions calculated using misorientation and orientation spread data in the next section. The percent below this cutoff density (ie. a lower average GND density) can be seen in Table 1.

EBSD Based Recrystallization

There are 3 methods which are most commonly used for general recrystallization analysis when using EBSD: the grain orientation spread (GOS), the grain average missorientation (GAM), and the kernal average misorientation (KAM). Each of these requires an angular threshold value to determine the level of recrystallization in the material. Through literature review 3 threshold values were found for GOS: 2.0°, 2.5°, and 3.0° [8-10], 1 value was found for GAM: 1.55° [11], and 1 value for KAM: 1.0° [10]. Based on these values, it was determined that the investigation should look at a wide range of threshold values (0.0° - 5.0°) in order to determine whether the values found would be useful in

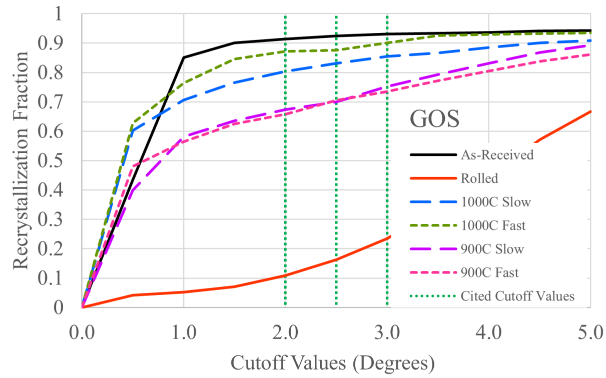

(a) GOS plot with cited cutoff values [8–10].

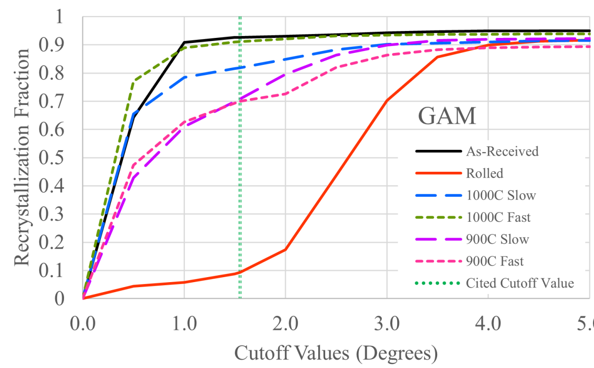

(b) GAM plot with cited cutoff values [11].

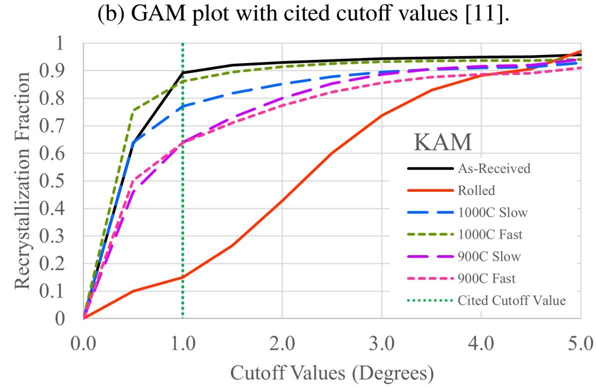

(c) KAM plot with cited cutoff values [10].

Figure 5: Recrystallization fraction of all samples calculated via EBSD analysis of GOS, GAM, and KAM.

determining the recrystallization in our samples. The implication of the threshold values can be seen in the GOS, GAM, and KAM plots shown in Fig. 5. For each method of recrystallization analysis a threshold below 3.5° is needed to ensure that the outcome is meaningful. It is also important to note that threshold values below 0.5° may be untrustwor-thy based on the accuracy limits of the EBSD techniques. Despite this the threshold values noted in the literature are in general agreement in predicting the recrystallization fraction for each sample. This can be seen in Fig. 6, in which the 5 threshold values are used to look at the spread of recrystal-lization within the sample. Each sample has an attributed error of ~5% with the 1000 ◦ C heat treatments having a slightly lower spread in values.

ISBN: 978-3-95450-233-2 ISSN: 2673-5504 doi:10.18429/JACoW-SRF2021-SUPCAV002

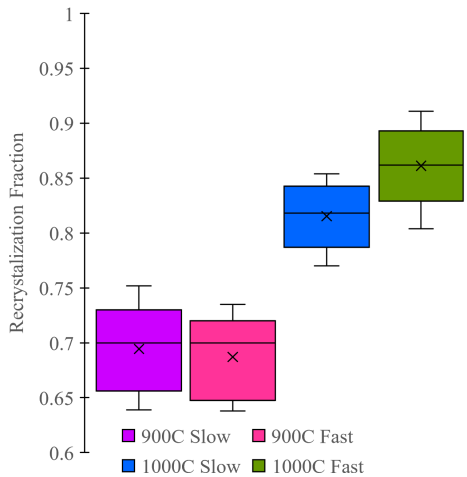

Figure 6: A box and whisker plot relating all of the cited values for GOS, GAM, and KAM recrystallization fractions.

CONCLUSION

The GND density and recrystallization fractions of 4 uniquely heat treated samples of deformed high-purity nio-bium have been investigated using EBSD methods, to iden-tify the influence of heating rate and temperature on the microstructure of the deformed metal.

It is clear that the influence of the heating rate was more prominent in the 1000°C heat treatment as the fast heat-ing rate provides about 5% higher fractino of recrystallized grains. While the spread between the 1000°C heating rate values and the increase in recrystallization fraction from slow to fast agrees with both of our hypotheses and the GND density spread shown in Table 1, the 900°C heat treatment is not senstive to the heating rate. In the GND density analysis it was evident that the fast heating rate reduced a greater portion of the GNDs however due to the spread in data and the median values being within 1% of each other it is more difficult to gain a full picture of the influence of the heating rate at 900°C.

The observations of sample recrystallization and changes in GND density in this work provides clear evidence of the importance of a common (standard) processing method-ology during the final heat treatment during SRF cavitiy fabrication. This information will be useful for developing acceptance criteria for niobium used to fabricate high Q nio-bium cavities, and it will also increase our understanding of recrystallization in niobium.

REFERENCES

[1] S. Posen *et al.*, "The effect of mechanical cold work on the magnetic flux expulsion of Niobium", arXiv:1804.07207, 2019.

[2] G. Ciovati and A. Gurevich, "Evidence of high-field radio-frequency hot spots due to trapped vortices in niobium cavities", *Phys. Rev. Spec. Top. Accel. Beams*, vol. 11, no. 12, p. 122001, 2008. doi:10.1103/PhysRevSTAB.11.122001

[3] M. Wang, D. Kang, and T.R. Bieler, "Direct observation of dislocation structure evolution in SRF cavity niobium using electron channeling contrast imaging", *J. Appl. Phys.*, vol. 124, p. 155105, 2018. doi:10.1063/1.5050032

[4] M. Wang, T. Bieler, S. Balachandran, S. Chetri, A. A. Polyanskii, and P. J. Lee, "Study of dislocation content near grain boundaries using electron channeling contrast imaging and its effect on the superconducting properties of Niobium", in *Proc. SRF'19*, Dresden, Germany, Jun.-Jul. 2019, pp. 876-880. doi:10.18429/JACoW-SRF2019-THP020

[5] R.D. Doherty *et al.*, "Current issues in recrystallization: a review", *Mater. Sci. Eng., A*. vol. 238, pp. 219-274, 1997. doi:10.1016/S0921-5093(97)00424-3

[6] G. Ciovati *et al.*, "Mechanical properties of niobium radio-frequency cavities", *Mater. Sci. Eng., A*, vol. 642, pp. 117-127, 2015. doi:10.1016/j.msea.2015.06.095

[7] T. R. Bieler *et al.*, "Physical and mechanical metal-lurgy of high purity Nb for accelerator cavities", *Phys. Rev. Spec. Top. Accel. Beams*, vol. 13, pp. 31002, 2010. doi:10.1103/PhysRevSTAB.13.031002

[8] J. Wang *et al.*, "Microstructure heredity of Inconel 718 nickel-based superalloy during preheating and following deformation", *Crystals*, vol. 10, p. 303, Apr. 2020. doi:10.3390/cryst10040303

[9] H. H. Bernardi *et al.*, "Microstructural stability of a Niobium single crystal deformed by equal channel angular pressing", *Mater. Res.*, vol. 20, p. 5, Sep. 2017. doi:10.1590/1980-5373-MR-2017-0288

[10] P.O. Malta *et al.*, "Static recrystallization kinetics and crystallographic texture of Nb-stabilized ferritic stainless steel based on orientation imaging microscopy", *Metall. Mater. Trans. A*, vol. 48, pp. 1288–1309, 2017. doi:10.1007/s11661-016-3935-3

[11] H. Mirzadeh, J.M. Cabrera, A. Najafizadeh, and P.R. Calvillo, "EBSD study of a hot deformed austenitic stainless steel", *Mater. Sci. Eng., A*, vol. 538, pp. 236-245, 2012. doi:10.1016/j.msea.2012.01.037